Applied Magnetic Resonance (2020) 51:1019–1029
https://doi.org/10.1007/s00723-020-01212-2

Applied
Magnetic Resonance

ORIGINAL PAPER

# ESE-Detected Molecular Motions of Spin-Labeled Molecules on a Solid Inorganic Surface: Motional Models and Onset Temperatures

**Elena A. Golysheva[1,2] · Rimma I. Samoilova[1] · Marta De Zotti[3] · Fernando Formaggio[3,4] · Marina Gobbo[3,4] · Sergei A. Dzuba[1,2]**

Received: 2 June 2020 / Revised: 29 June 2020 / Published online: 24 July 2020


## Abstract

Electron spin echo (ESE) decays are highly sensitive to stochastic librations which are a general property of molecular solids of various origins. Adsorption of spin-labeled molecules on a solid inorganic surface under diluted conditions allows studying the motion devoid of the effects of cooperativity. Here, the temperature dependence of the motion-induced spin relaxation was studied for different types of spin-labeled molecules adsorbed on a $SiO_2$ surface. The spin relaxation rate for all the systems was found to attain well-defined maxima, which is in agreement with the model of uniaxial molecular librations. For spin-labeled stearic acid, the enhanced maximal relaxation rate was found which was interpreted as manifestation of two-axial (or planar) motion that is naturally expected for long flexible molecules. The data obtained suggest that the onset of the motions observed at two different temperatures, 100 K and 130 K, may be attributed to torsional and bending types of the motion, respectively. The models of non-cooperative motion developed for adsorbed molecules may become useful for analyzing motions in complex biological media, frozen ionic liquids, polymers, etc.

✉ Sergei A. Dzuba
dzuba@kinetics.nsc.ru

[1] Institute of Chemical Kinetics and Combustion, Russian Academy of Sciences, Novosibirsk 630090, Russian Federation

[2] Department of Physics, Novosibirsk State University, Novosibirsk 630090, Russian Federation

[3] Department of Chemical Sciences, University of Padova, 35131 Padova, Italy

[4] Institute of Biomolecular Chemistry, Padova Unit, CNR, 35131 Padova, Italy

## 1 Introduction

Electron spin echo (ESE) spectroscopy allows to detect stochastic molecular librations of spin-labeled species in molecular solids. This type of motion dominates at low temperatures where translational and rotational types of motion are suppressed. It was detected by measuring ESE decays in biological objects of different origin: frozen photosynthetic reaction centers [1], membranes [5], peptides and proteins [12], living seeds [20]. Also, it was found in polymers [21] and molecular glasses [22] including frozen ionic liquids [25, 26].

The high-field EPR which was pioneered by Lebedev [27] benefits from a higher sensitivity to the molecular reorientations [1, 2]. This high sensitivity allows intramolecular motions also to be detected [28].

The study of stochastic librations may be used to derive information on the nanostructure of lipid bilayers [5, 11, 13, 29–31], polymers [21] and ionic liquids [26], on the nature of dynamical transitions in membranes and proteins [4, 7, 11, 19, 32], on the molecular mechanisms of protein and peptide action [12, 33], on the internal flexibility of the molecules [28].

In biological media, in polymers and molecular glasses the motions occur in a cage in which the molecule is encapsulated, and a cooperative rearrangement of this cage [34] may also contribute to the ESE decays. To get deeper insight into the molecular mechanisms determining this type of motion, it is reasonable to devise experiments in which only individual motions of the molecules may appear. Cooperative effects certainly can be ruled out for molecules adsorbed at low concentrations on solid inorganic surfaces, such as $SiO_2$. It was found [35] that the spin relaxation induced by stochastic librations on $SiO_2$ surface increases with temperature until it attains its maximum, which was found to be the same for both a small nitroxide and a large spin-labeled peptide. This maximal value is reproduced fairly well in theoretical simulations assuming uniaxial stochastic librations [35].

To get additional support for the general applicability of the conclusions drawn in [35] about spin relaxation, in this work we study stochastic molecular librations for different types of spin-labeled molecules absorbed on a $SiO_2$ surface. Increasing the range of the systems investigated resulted in qualitatively new results, which allowed gaining deeper insight into the mechanisms of ESE-detected stochastic molecular librations.

## 2 Experimental

### 2.1 Materials and Samples

Different types of spin probes and spin-labeled molecules were used (Fig. 1): nitroxides **I** and **II**, two **TOAC**-spin-labeled analogs of antibiotic peptides, alamethicin (alaTOAC16) and tylopeptin (tyloTOAC13), in which **TOAC** replaces a

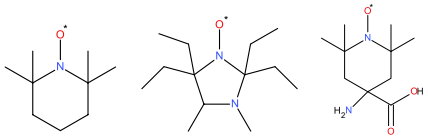

**I (TEMPO)** **II** **TOAC**

Ac-Aib[1]-Pro-Aib[3]-Ala-Aib[5]-Ala-Glu(OMe)-Aib[8]-Val-Aib[10]-Gly-Leu-Aib[13]-Pro-Val-**TOAC**[16]-Aib[17]-Glu(OMe)-Glu(OMe)-Phl (alaTOAC16)

Ac-Trp-Val-Aib[3]-Aib[4]-Ala-Gln-Ala-Aib[8]-Ser-Aib[10]-Ala-Leu-**TOAC**[13]-Gln-Lol (tyloTOAC13)

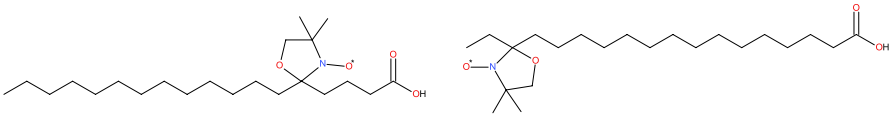

5-DOXYL-stearic acid (5-DSA) 16-DOXYL-stearic acid (16-DSA)

**Fig. 1** Chemical structures of the six molecules used in this study

residue of $\alpha$-aminoisobutyric acid (Aib), and spin-labeled 5- and 16-DOXYL-stearic acid (5-DSA and 16-DSA, respectively).

Nitroxide **I**, 5-DSA and 16-DSA were purchased from Sigma-Aldrich (Saint Louis, MO, USA). Nitroxide **II** was kindly provided by Kirilyuk (Novosibirsk). Synthesis, purification and chemical characterization of the spin-labeled peptides alaTOAC16 [36] and tyloTOAC13 [37] were previously described. The colloidal silica powder (ZAO Polisorb, Chelyabinsk region, RF) consists of monodisperse spherical particles of 20 nm diameter [38].

The adsorption process was achieved by putting the silica powder on an Amicon Ultrafree-MC Durapore PVDF centrifugal filter (Millipore, MA, USA) and adding a methanol solution of a spin-labeled substance. After letting 30 min for the adsorption to proceed, non-adsorbed matter and solvent were removed by centrifugation (2000 rpm, 4 min, 20 °C). The sample was dried by means of an argon stream and put into a 3 mm EPR glass tube. Then, air was pumped out ($10^{-3}$ torr) and the tube was sealed.

### 2.2 EPR/ESE Measurements

The measurements of continuous wave (CW) EPR spectra, echo detected (ED) EPR spectra and of ESE decays were performed on an X-band ELEXSYS 9-GHz FT-EPR spectrometer (Bruker, Bremen, Germany) equipped by CF 935 cryostat (Oxford instruments, Abingdon, UK) with a split-ring resonator Bruker ER 4118X-MS3 inside. The temperature was controlled by a cold nitrogen stream with an accuracy of $\pm 0.5$ K. The CW experiments were conducted under conditions avoiding

overmodulation and saturation. In the pulsed experiments the resonator cavity was overcoupled to provide a ringing time of about 100 ns. A two-pulse sequence (90º-$\tau$-180º-$\tau$-echo) was used. Pulse durations were 16 ns and 32 ns for 90º- and 180º-pulses, respectively. The time delay $\tau$ was scanned starting from 120 ns with a step of 4 ns. Echo-detected (ED) EPR spectra were recorded with time delay $\tau$ kept constant (120 ns).

## 3 Results

CW EPR spectra recorded at room temperature for all samples are shown in Fig. 2. They correspond to those typically found for immobilized nitroxides, except for **I** and **II** which demonstrate some mobility. For all other systems, spectra in Fig. 2 reflect the anisotropic nature of magnetic interactions determining the EPR lineshape (anisotropy of both g-factor and hyperfine interaction).

Extra line broadening, diagnostic of molecular aggregation, is not observed in any spectra. In this respect, ESE data we recently obtained [35] under similar experimental conditions allowed us to estimate a distance between the molecules on the surface as ~ 10 nm, which is much larger than the molecular sizes of the molecules used in this study. Therefore, the adsorbed molecules on the surface indeed can be considered diluted. (Note that quantities of the spin-labeled molecules estimated from intensity of the EPR spectra before and after adsorption were approximately of the same order.)

Examples of ED EPR spectra are shown in Fig. 3 for the 16-DSA/$SiO_2$ system. The spectra were obtained at different temperatures with time $\tau$ kept constantly equal to 120 ns. The spectra are normalized to the central peak (position 1 in Fig. 3),

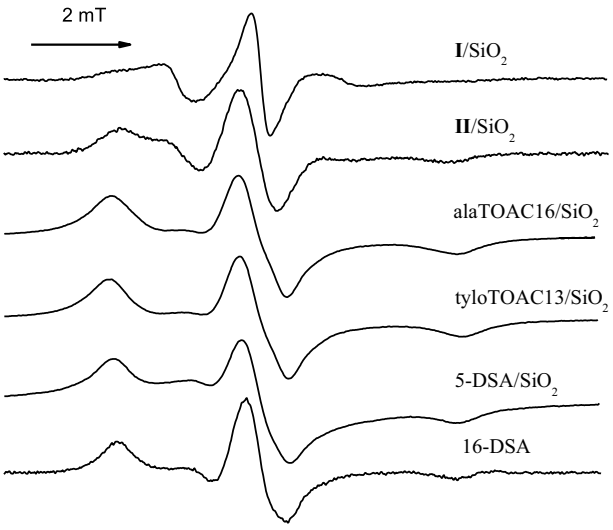


**Fig. 2** CW EPR spectra at room temperature for the spin-labeled molecules adsorbed on the $SiO_2$ surface

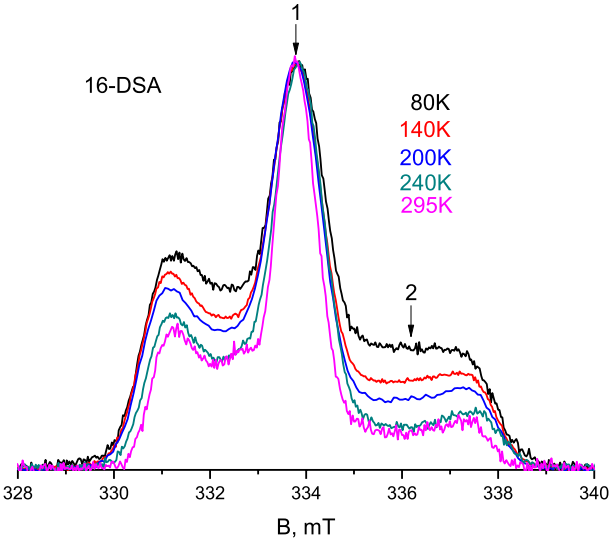


**Fig. 3** ED EPR spectra for the 16-DSA/$SiO_2$ sample taken with the same time delay $\tau = 120$ ns at different temperatures. Spectra are normalized to the same amplitude of the central component (position 1), to visualize the anisotropic nature of spin relaxation which proceeds with the highest rate in the middle of the most anisotropic component (position 2)

to exclude field-independent spin relaxation mechanisms, and to visualize the anisotropic nature of spin relaxation. One can see that relaxation at the middle of the high-field component (position 2) becomes faster with increasing temperature. Conversely, relaxation of the two outer shoulders is relatively slow, as expected for spin-relaxation induced by stochastic molecular librations [5–9].

The theoretical characterization of ESE decay induced by stochastic librations has been described in detail elsewhere [5–9]. The model of stochastic librations predicts an exponential decay of the echo amplitude $E(2\tau)$ as the time delay $\tau$ between two pulses increases. This exponential behavior is indeed observed. As an example, Fig. 4 reports for 16-DSA/$SiO_2$ the ratio between the two echo decays $E_2(2\tau)$ and $E_1(2\tau)$, taken at field positions 1 and 2 (see Fig. 3), respectively.

The ratio between the two decays, $E_2(2\tau)/E_1(2\tau)$, plotted in a semilogarithmic scale allows to get the motion-related relaxation rate, $\Delta W$, as the slope given in Fig. 4b. According to the theory [5–9], the ratio of two ESE decays obtained at two field positions can be expressed as

$$E(2\tau) = \frac{E_2(2\tau)}{E_1(2\tau)} = const exp(-2\tau\Delta W). \quad (1)$$

The results of such data treatment applied to the different systems studied are presented in Fig. 5 where the $\Delta W$ temperature dependence is shown. We note that $\Delta W$ starts to increase above 100 K for 5-DSA/$SiO_2$ and above ~ 130 K for all other samples. Above ~ 200 K the $\Delta W$ increase becomes slower until a plateau is attained

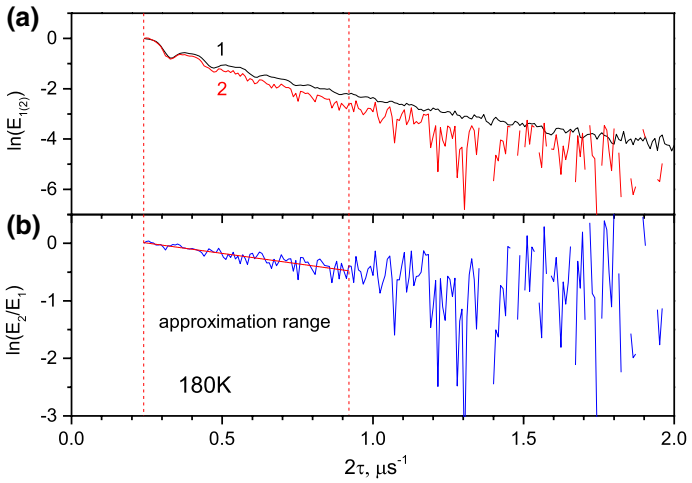


**Fig. 4** Semi-logarithmic plot for: **a** ESE decays at field positions 1 and 2 (see Fig. 3); **b** the ratio between the two decays (acquired for 16-DSA/$SiO_2$ at 180 K). Two dashed lines denote the time range chosen for a linear approximation (shown by a solid straight red line)

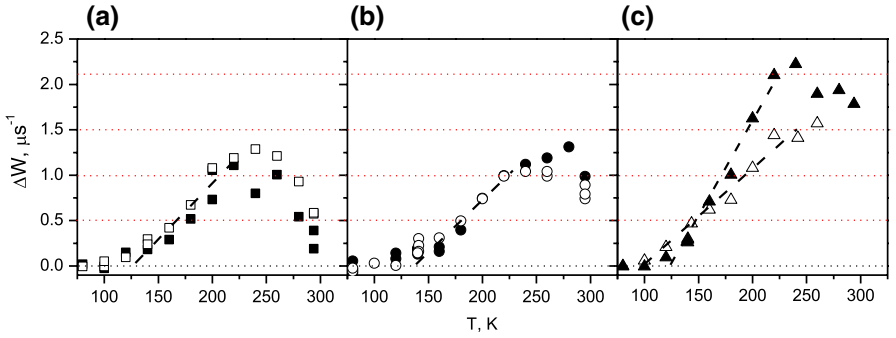


**Fig. 5** Temperature dependence of anisotropic relaxation rate $\Delta W$ for the samples: **a I** (TEMPO)/$SiO_2$ (filled squares), **II**/$SiO_2$ (open squares); **b** alaTOAC16/$SiO_2$ (filled circles) and tyloTOAC13/$SiO_2$ (open circles); **c** for the 16-DSA/$SiO_2$ (filled triangles) and 5-DSA/$SiO_2$ (open triangles). The dashed lines are linear data approximations (see text)

at about 250 K, with subsequent tendency to a $\Delta W$ decrease. The maximum $\Delta W$ value observed for **I**/$SiO_2$, **II**/$SiO_2$, alaTOAC16/$SiO_2$ and tyloTOAC13/$SiO_2$ is about 1 $\mu s^{-1}$ (see Fig. 5a, b). The maximum $\Delta W$ values for 16-DSA/$SiO_2$ and 5-DSA/$SiO_2$ are about $2 \pm 0.05$ and $1.5 \pm 0.1$ $\mu s^{-1}$, respectively (Fig. 5c).

The dashed lines drawn in Fig. 5 are linear data approximations starting from the onset of the $\Delta W$ and increasing up to the $\Delta W$ value for which the plateau is attained. The x-intercepts of these lines allow to obtain an onset temperature, $T_0$, namely the starting temperature for the molecular motion in this experiment. One can see that $T_0$ falls near 100 K for the 5-DSA/$SiO_2$ sample and lies between 125 and 135 K for all other systems.

## 4 Discussion

The CW EPR spectra at room temperature (Fig. 2) for **I**/$SiO_2$ and **II**/$SiO_2$ correspond to nitroxides with some mobility detectable in the CW EPR timescale. We may explain this mobility with a relatively weak bonding between the nitroxides and the surface. Then free rotation at room temperature may become the cause of a dramatic decrease in the anisotropic relaxation rate close to room temperature, as seen in Fig. 5a.

ESE decays measured in a wide temperature range were successfully simulated [35] using a simple two-site model [39] of random jumps by angles $\pm\alpha$ around an axis lying in the *xy*-plane of the molecular frame. This simplification of the real stochastic libration dynamics benefits from reproducing ESE decays for arbitrary angles $\alpha$ and correlation times $\tau_c$. In the case of fast motions [$(< \Delta\omega^2(t) > \tau_c^2 \ll 1)$, where $\Delta\omega$ is the resonance frequency fluctuation due to the motion which is directly related to $\alpha$], the simulated ESE decay is reduced to an exponential dependence$E(2\tau) = exp(-2\tau\Delta W)$, where $\Delta W = \Delta\omega^2\tau_c$. This result is in agreement with that obtained with the model of stochastic librations [5–9]. However, for large $\Delta\omega$, the $\Delta W$ value in the two-site model attains a maximum that is independent of $\alpha$. The calculations therefore explain the experimental saturating behavior of the $\Delta W$ temperature dependence. Quantitative agreement with the experimental data was also achieved [35].

The $\Delta W$ temperature dependence found here (Fig. 5) resembles the one previously obtained for two other types of molecules adsorbed on $SiO_2$ surface [35]: nitroxide **III** and the spin-labeled antibiotic peptide trichogin GA (triTOAC4) (Fig. 6, where *n*Oct is *n*-octanoyl and Lol is the 1,2-amino alcohol leucinol). In both cases $\Delta W$ reached a plateau as the temperature increased, with $\Delta W_{max} \approx 1\ \mu s^{-1}$ for triTOAC4/$SiO_2$ and $\approx 1.5\ \mu s^{-1}$ for **III**/$SiO_2$ and $T_0 \approx 130$ K in both cases.

Theoretical simulations [35] showed that the limiting value $\Delta W_{max} \approx 1\ \mu s^{-1}$ is reproduced by the model of *uniaxial* librations around an axis lying in the *xy*-plane of the nitroxide molecular frame. If one assumes that librations may occur independently around two different axes, then the relaxation rates induced by these two types of motion should be multiplied, which implies that $\Delta W_{max} \approx 2\ \mu s^{-1}$. This explains the data observed here for the 16-DSA/$SiO_2$ system (Fig. 5c).

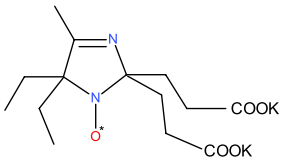


**III**

*n*Oct-Aib-Gly-Leu-**TOAC**-Gly–Gly-Leu-Aib-Gly-Ile-Lol (triTOAC4)

**Fig. 6** Chemical structure of nitroxide III and amino acid sequence of triTOAC4 studied in [35]

Note that calculation [35] shows that the $\Delta W_{max}$ value is also doubled if the correlation time $\tau_c$ becomes larger than 100 ns (see Fig. 7 in [35]). However estimations for correlation time $\tau_c$ for ESE-detected librational motion [5, 7, 12, 19, 32] indicate that $\tau_c$ lies in nanosecond time scale so this possibility may be certainly ruled out.

16-DSA is most probably linked to the $SiO_2$ surface through its carboxyl group and the nitroxide moiety at the other end of the molecule. The long aliphatic tail at low temperatures possesses an extended *trans*-conformation, at least in the vicinity of the spin label. The aliphatic tail, because of its length and relatively week adsorption, may freely move in two directions perpendicular to its axis. Driven by this motion, the nitroxide is expected to perform independent motions also around two axes in the *xy* molecular plane of the nitroxide (*two-axial* libration); or a *planar* libration within a cone [2].

For the 5-DSA molecule bound to the $SiO_2$ surface, some restrictions to this two-axial motion may occur, because of the closeness of the nitroxide moiety to the highly-polar carboxyl group, which is expected to be strongly coupled to the surface. So, the $\Delta W_{max} \approx 1.5\ \mu s^{-1}$ found here may be explained as an intermediate situation between uniaxial and two-axial motions. In this respect, the structure of **III** looks similar to that of 5-DSA one (cf. Figs. 1 and 6); this structural similarity explains the close value for $\Delta W_{max} \approx 1.5\ \mu s^{-1}$ observed for **III**/$SiO_2$ [35] and 5-DSA/$SiO_2$ (Fig. 5c).

The temperature $T_0$, obtained in Fig. 5, marks the onset of the motion. $T_0$ is near 100 K for the 5-DSA/$SiO_2$ system and lies between 125 and 135 K for all other systems. It is interesting to note that literature data also evidence that, depending on the system, ESE-detected stochastic librations appear either near 100 K or near 130 K. The case of $T_0 \approx 100$ K was found for spin-labeled stearic acids interacting with membranous Na,K-ATPase [13], for spin-labeled phospholipids in DPPC/

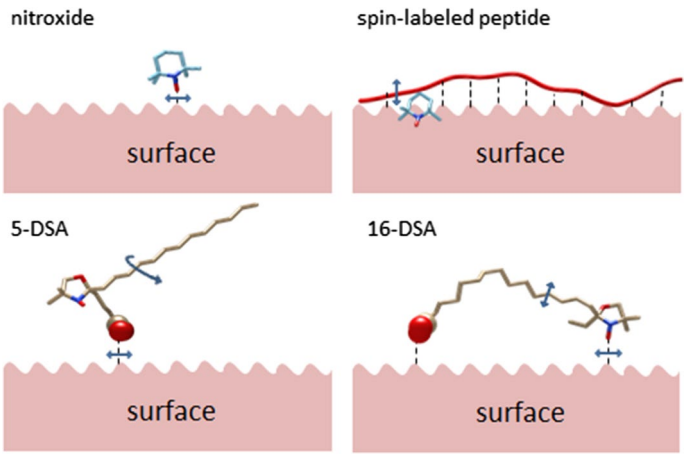


**Fig. 7** Schematic presentation of different motional types experienced by spin labels: uniaxial bending motions for nitroxides **I** and **II** and for spin-labeled peptide alaTOAC16, two-axial bending motions for 5-DSA and for 16-DSA. In the case of 5-DSA, the motion of spin label may be influenced by torsional motion of the free aliphatic tail

Cholesterol (50:50 mol%) bilayer [5], for antimicrobial peptide alamethicin spin-labeled at positions 8 and 16 of the amino acid sequence and bound to a phospholipid bilayer [12], for spin probe in dry lysozyme [19], for frozen ionic liquids [25, 26] (here motions appear between 80 and 100 K), for spin-labeled molecules in bilayer formed by unsaturated phospholipids [11, 32]. The case of $T_0 \approx 130$ K was found for spin-labeled molecules in bilayers of fully saturated phospholipids [7, 32], for antimicrobial peptide alamethicin spin-labeled at position 1 and bound to a phospholipid bilayer [12], and for hydrated spin-labeled lysozyme [19].

Figure 7 shows the schematic presentation of motional types which may appear for the systems studied here. Librational motions of the molecules coupled to the surface may be of two types, bending and torsional ones [40]; both types may be either uniaxial or two-axial. For nitroxides **I** and **II** only uniaxial bending motion relative to their bonds to the surface is expected, because of restrictions imposed by anisotropy of the bonding potential. For spin-labeled peptides, the uniaxial bending motion may appear relative to the peptide bonds. In the cases of 5-DSA and 16-DSA, the spin label may perform two-axial bending motion because of flexibility of the long aliphatic tail (with some restrictions in the case of 5-DSA—see above). And 5-DSA differs from all the others by the presence of free aliphatic tail, which may perform torsional motion. The influence of torsional motion on the motion of spin label may explain why for the 5-DSA/$SiO_2$ system $T_0 \approx 100$ K while in all the other systems $T_0 \approx 130$ K: for these systems the torsions are damped and therefore bending motions dominate.

The hypothesis of prevalence either of torsional or bending motions may be confirmed by Raman scattering data for bilayers composed of unsaturated and saturated phospholipids [30]. Indeed, torsional motions of the lipid aliphatic tails are expected to be coupled with antisymmetric H-C-H group vibration in these tails, because of the same local symmetry for the both types of these motions. Raman scattering data for antisymmetric H-C-H group vibration [30] show for unsaturated lipids line broadening starting near ~ 100 K, while for saturated lipids the line broadening starts at much higher temperatures (near 170 K). This observation may be explained by the looser lipid packing in the former case which allows the torsional motions to evolve along the aliphatic chain, while in the latter case torsions may be damped because of the denser packing. Meanwhile, there was found that for stochastic librations $T_0 \approx 100$ K for unsaturated lipids and $T_0 \approx 130$ K for saturated lipids [32]; this coincidence of two temperatures (100 K) in two different experiments, [30] and [32], indeed may confirm importance of torsional motions for free aliphatic tails.

## 5 Conclusions

The study of ESE-detected motions for spin-labeled molecules adsorbed on a solid surface allows to refine the contribution of individual non-cooperative motions. Results of the studies performed in the present work show that maximal spin relaxation rate observed in ESE decays is enhanced for highly flexible molecules, like stearic acid. This rate enhancing was interpreted as a result of two-axial (or planar) motion appearing instead of the uniaxial motion typical for more rigid molecules.

The results obtained here also suggest that the onset of ESE-detected librational motions takes place near 130 K for systems where only bending motions may be expected, whereas if the molecules have enough length and intermolecular freedom for torsional motion, librations appear already at a temperature of about 100 K.

In general, the data obtained may help in the analysis of ESE-detected stochastic molecular librations in frozen biological media, frozen ionic liquids, polymers and other molecular solids.

**Acknowledgements** This work was jointly supported by the Russian Foundation for Basic Research and by the Government of Novosibirsk Region, project # 18-43-540004. MDZ gratefully acknowledge the financial support by University of Padova (project P-DiSC#04BIRD2019-UNIPD) and by MIUR (PRIN2017 project n. 20173LBZM2).

## References

1. A. Schnegg, M. Fuhs, M. Rohrer, W. Lubitz, T.F. Prisner, K. Möbius, J. Phys. Chem. B **106**, 9454 (2002)
2. O.G. Poluektov, L.M. Utschig, S. Dalosto, M.C. Thurnauer, J. Phys. Chem. B **107**, 6239 (2003)
3. A. Savitsky, K. Möbius, Photosynth. Res. **102**, 311 (2009)
4. I.V. Borovykh, P. Gast, S.A. Dzuba, Appl. Magn. Reson. **31**, 159 (2007)
5. D.A. Erilov, R. Bartucci, R. Guzzi, D. Marsh, S.A. Dzuba, L. Sportelli, Biophys. J. **87**, 3873 (2004)
6. D.A. Erilov, R. Bartucci, R. Guzzi, D. Marsh, S.A. Dzuba, L. Sportelli, J. Phys. Chem. B **108**, 4501 (2004)
7. E. Aloi, M. Oranges, R. Guzzi, R. Bartucci, J. Phys. Chem. B **121**, 9239 (2017)
8. N.P. Isaev, S.A. Dzuba, J. Phys. Chem. B **112**, 13285 (2008)
9. K.B. Konov, N.P. Isaev, S.A. Dzuba, J. Phys. Chem. B **118**, 12478 (2014)
10. F. De Simone, R. Guzzi, L. Sportelli, D. Marsh, R. Bartucci, Biochim. Biophys. Acta **1768**, 1541 (2007)
11. E. Aloi, R. Guzzi, R. Bartucci, Phys. Chem. Chem. Phys. **21**, 18699 (2019)
12. R. Bartucci, R. Guzzi, M. De Zotti, C. Toniolo, L. Sportelli, D. Marsh, Biophys. J. **94**, 2698 (2008)
13. R. Guzzi, R. Bartucci, M. Esmann, D. Marsh, Biophys. J. **108**, 2825 (2015)
14. R. Guzzi, M. Babavali, R. Bartucci, L. Sportelli, M. Esmann, D. Marsh, Biochim. Biophys. Acta **1808**, 1618 (2011)
15. F. Scarpelli, R. Bartucci, L. Sportelli, R. Guzzi, Eur. Biophys. J. **40**, 273 (2011)
16. H.-J. Steinhoff, A. Savitsky, C. Wegener, M. Pfeiffer, M. Plato, K. Möbius, Biochim. Biophys. Acta **1457**, 253 (2000)
17. A. Volkov, C. Dockter, T. Bund, H. Paulsen, G. Jeschke, Biophys. J. **96**, 1124 (2009)
18. V.S. Oganesyan, Phys. Chem. Chem. Phys. **13**, 4724 (2011)
19. E.A. Golysheva, G.Y. Shevelev, S.A. Dzuba, J. Chem. Phys. **147**, 064501 (2017)
20. S.A. Dzuba, Y.A. Golovina, Yu.D. Tsvetkov, J. Magn. Reson. B **101**, 134 (1993)
21. D. Leporini, G. Jeschke, Philos. Mag. **84**, 1567 (2004)
22. S.A. Dzuba, Yu.D. Tsvetkov, A.G. Maryasov, Chem. Phys. Lett. **188**, 217 (1992)
23. E.P. Kirilina, S.A. Dzuba, A.G. Maryasov, Yu.D. Tsvetkov, Appl. Magn. Reson. **21**, 203 (2001)
24. E.P. Kirilina, T.F. Prisner, M. Bennati, B. Endeward, S.A. Dzuba, M.R. Fuchs, K. Möbius, A. Schnegg, Magn. Reson. Chem. **43**, S119 (2005)
25. M.Y. Ivanov, O.A. Krumkacheva, S.A. Dzuba, M.V. Fedin, Phys. Chem. Chem. Phys. **19**, 26158 (2017)
26. M.Y. Ivanov, S.A. Prikhod'ko, N.Y. Adonin, I.A. Kirilyuk, S.V. Adichtchev, N.V. Surovtsev, S.A. Dzuba, M.V. Fedin, J. Phys. Chem. Lett. **9**, 4607 (2018)
27. Y.S. Lebedev, Appl. Magn. Reson. **7**, 339 (1994)
28. A. Savitsky, M. Plato, K. Möbius, Appl. Magn. Reson. **37**, 415 (2010)
29. N.P. Isaev, V.N. Syryamina, S.A. Dzuba, J. Phys. Chem. B **114**, 9510 (2010)
30. N.V. Surovtsev, N.V. Ivanisenko, K.Y. Kirillov, S.A. Dzuba, J. Phys. Chem. B **116**, 8139 (2012)

31. E.A. Golysheva, S.A. Dzuba, Chem. Phys. Lipids **226**, 104817 (2020)
32. E.A. Golysheva, M. De Zotti, C. Toniolo, F. Formaggio, S.A. Dzuba, Appl. Magn. Reason. **49**, 1369 (2018)
33. V.N. Syryamina, N.P. Isaev, C. Peggion, F. Formaggio, C. Toniolo, J. Raap, S.A. Dzuba, J. Phys. Chem. B **114**, 12277 (2010)
34. E. Meirovitch, A. Nayeem, J.H. Freed, J. Phys. Chem. **88**, 3454 (1984)
35. E.A. Golysheva, R.I. Samoilova, M. De Zotti, C. Toniolo, F. Formaggio, S.A. Dzuba, J. Magn. Reson. **309**, 106621 (2019)
36. C. Peggion, M. Jost, C. Baldini, F. Formaggio, C. Toniolo, Chem. Biodivers. **4**, 1183 (2007)
37. M. Gobbo, E. Merli, B. Biondi, S. Oancea, A. Toffoletti, F. Formaggio, C. Toniolo, J. Pept. Sci. **18**, 37 (2012)
38. V.N. Syryamina, R.I. Samoilova, Y.D. Tsvetkov, A.V. Ischenko, M. De Zotti, M. Gobbo, C. Toniolo, F. Formaggio, S.A. Dzuba, Appl. Magn. Reson. **47**, 309 (2016)
39. K.M. Salikhov, S.A. Dzuba, A.M. Raitsimring, J. Magn. Reson. **42**, 255 (1981)
40. F.Y. Hansen, J.C. Newton, H. Taub, J. Chem. Phys. **98**, 4128 (1993)